Proceedings World Geothermal Congress 2010
Bali, Indonesia, 25-29 April 2010

Hydrogeochemistry of Geothermal Resources in the Eastern Part of Turkey: A Case Study, Varto Region

[1]Alper Baba, [2]Erdinç Yiğitbaş and [2]Can Ertekin

[1]Izmir Institute of Technology, Engineering Faculty, 35430, Urla, Izmir, TURKEY, E-mail: alperbaba@iyte.edu.tr

[2]Çanakkale Onsekiz Mart University, Engineering & Architectural Faculty, Geological Eng Dept, 17020, Çanakkale, Turkey

Keywords: hydrogeochemistry, geothermometers, Varto, Turkey.

ABSTRACT

Varto, in the eastern part of Turkey, is settled around the conjunction point of the East Anatolian (EAF) and North Anatolian (NAF) Fault zones. The border of these tectonic zones constitutes seismic belts marked by young volcanic associations and active faults, the latter allowing circulation of waters as well as heat. For this reason, there are various geothermal systems having several hot water springs in the region. The distribution of hot water springs in the Varto Region roughly parallels the distribution of the fault systems and young volcanism. Samples from five hot water and two mineral water springs together with cold (peripheral) waters were collected. Hot water samples were assessed through geothermometers in terms of geothermal usage opportunities. All water samples were measured and analyzed for physical, chemical and isotopic compositions. Physical parameters such as pH, electrical conductivity (EC; µS/cm) and temperature (T; ºC) were measured in field. Primary (major ions) and secondary constituents (trace elements and heavy metals) and Oxygen 18 (^{18}O), Deuterium (D), Tritium (^{3}H) isotopic compositions were determined by mass spectrometry. Average discharges of hot water springs in the study area are between 1 - 5 L/sec. Surface temperatures of these springs vary 22.5 to 32ºC, electrical conductivity (EC) values 2100 to 5775µS/cm. Average discharges of mineral waters in that site are between 0.5 - 2 L/sec. Surface temperatures of them were measured as 13.2 and 14.8ºC. Their electrical conductivity values are also in the range of 719 - 751 µS/cm. The average discharges of cold water springs in the study area are between 1 - 150 L/sec. Surface temperatures of these springs change between 4.9 - 11.7ºC and electrical conductivity values 51 - 199 µS/cm. Regarding pH values, water samples belonging to the site are entirely distinguished into the pH range of ~5.4 - ~6.2 for hot and mineral waters, ~6.2 - ~7.7 for cold waters. Hot water springs have acidic character, whereas pH values of cold water springs change from slightly acidic to neutral and slightly basic. In the vicinity of the study area, volcanic and volcaniclastic rocks crop out. Groundwater flow in the volcanic rocks is also controlled by the presence of structural features as suggested by the alignment of the springs. Their cooling fractures extend several meters in depth, providing a good avenue for deep penetration and circulation of groundwater. According to the Piper diagram, springs fall into Na-HCO_3-Cl type for thermal waters and Ca-HCO_3 type for cold waters. Due to the fractures allowing deep circulation of groundwater and dominant Na-Cl component, the host rock is probably volcanic origin. Hot waters have the same recharge area with cold waters. The information on the fluid origin and the age of springs depicted by their ^{18}O-D and T contents shows that they are all meteoric origin and hot water springs are older than 50 years. Reliable reservoir temperature ranges for hot waters were obtained with Li-Mg geothermometer and β-Cristobalite geothermometer as 44 - 66ºC and 54 - 80ºC, respectively. These values are also checked with Saturation Indices (SI) *vs* T diagrams. Results of SI *vs* T diagrams point out equilibration with calcite and aragonite minerals which gives comparable results with Li-Mg and β-Cristobalite geothermometers. It is possible to get 80°C reservoir temperature by drilling in this area with the help of field observations and the data obtained. The geothermal potential of the study area have not been used up to now. This geothermal district might make a considerable contribution to tourism and agriculture usages.

1. INTRODUCTION

Geothermal fields are segregated into active tectonic zones throughout the world in a range of different geological settings. As being peculiar characteristics, geological settings reflect the chemistry of the geothermal fluids and their potential applications. Geochemistry gives answers to the broad range of questions that arise from all stages of the exploration, evaluation and exploitation of geothermal fields. In the exploration stage, the appraisal of geochemistry is connected with the judgment of specifying fluid types (water and vapor phase or both), sources (origins) and reservoir temperatures. Regarding the exploration stage, this paper is confined with exploratory hydrogeochemistry (just meaning aqueous chemistry here) of thermal springs of Varto, in the eastern Turkey.

The geothermal scheme of Turkey is diminished in scope in Fig. 1. Spatial extension of geothermal springs and fields are strewn with volcanics of Upper Tertiary-Quaternary and lies throughout especially the active faults of the North Anatolian Fault (NAF) and the East Anatolian Fault (EAF). In this scheme, The Varto Region is settled around the conjunction point of NAF and EAF (Fig. 1). The border of these tectonic zones constitutes seismic belts marked by volcanics and the active faults, the latter allowing circulation of waters as well as heat. Notwithstanding being known surface manifestations of the thermal springs, the region is untouched. For that reason, the exploratory base study was launched and its immediate consequences are introduced here.

Figure 1: The Geothermal map of Turkey and the Varto region (modified Şimşek, 1997).

2. THE SITE DESCRIPTION

The Varto Region is settled in the eastern part of Turkey (Fig. 1), living a population of approximately 10,800 inhabitants. The nearest large population center to the Varto Region is the provincial capital city of Muş with an approximately population of 80,000. Modes of the commercial settings are uniform, significantly sheep-goat herding and less extensively agriculture. Due to this uniform view, usage of the geothermal potential can serve directly the local economy in the meaning of augmentation employment of that region. For this purpose, exploratory hydrogeochemistry of geothermal springs is needed. Thermal and mineral-cold springs considered are situated throughout the northwestern part of the region and also cover a spatially small portion of it as seen in Fig. 2.

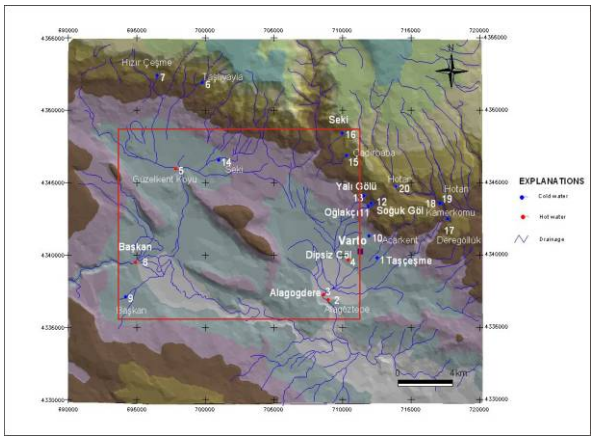

Figure 2: The geothermal site (marked with red).

Consequently, this fact yields using terms of the site or the study field, indicating only discharging area of springs, hereafter in this text. Spatially, the site extends 41° 14' 50" to 41° 31' 28" in easting and 39° 09' 39" to 39° 17' 40" in northing (Fig. 2). In the first step, on-site measurement and sample treatment are performed in this site. In the second step, exploratory base of aqueous chemistry data was handled. An explanation covering two steps of methodology is given in the following section.

3. METHODS

The sampling campaign in this field was performed for five hot water and two mineral water springs together with cold (peripheral) waters in November 2008. On-site measurements include physical parameters of pH, electrical conductivity (EC; µS/cm), temperature (T; ºC), redox potential (Eh; mV) and flow rate (Q; L/s). About sample treatment, 0.45 µm filter membranes were placed to the top of each vessel when collecting groundwater samples. Double-tapped plastic vessels of 50 mL were used and filled with water to the extent that overflowing is preserved. In order to prevent complex formation of heavy metals with oxygen, pH<2 conditions were maintained. These types of samples were used for primary (major ions) – secondary constituents (trace elements and heavy metals). 100 mL water was stored into plastic vessels as unacidified for ^{18}O and D. For ^{3}H determination, unacidifed water samples of 1 L were collected. Concentrations and isotopic compositions of all samples were determined by mass spectrometry.

The data handling was performed by the descriptive manner of specifying water types (facies), their origins and average reservoir (host) rock temperature calculation. Piper and Schoeller diagrams are used to emphasize differences and similarities in terms of water types. Isotopic signatures of samples indicate their origins. Solute geothermometer equations were applied to calculate average reservoir rock temperatures.

Every step of the data handling is explained in separate sections below, but the surface geology of the region is firstly introduced in the following section. The reason why surface geology is the first place is that it gives a way to interpret in some depths of subsurface geology that appear to be useful identifying water-rock interaction affecting ascending geothermal fluids, and is important for confident application of geothermometers, predicting scaling-corrosion issues as well.

4. GEOLOGICAL BACKGROUND OF THE VARTO REGION

In the upper view, The Varto Region sets into the Eastern Anatolia. This part of Anatolia is called the Eastern Anatolia High Plateau belonging to the Turkish-Iranian Plateau, more than half of the area lying at the elevation of about 1.5km. Young volcanic cones formed as conspicuous peaks are distinctive morphological features of the Eastern Anatolia and the Varto Region. The Neo-Tethyan to Quaternary geological evolution of the Eastern Anatolia and the Varto Region is just touched upon in the rest of this section.

In the Eastern Anatolia, the latest oceanic lithosphere of the Tethyan oceanic realm was eliminated when the Arabian platform initiated to collide with Laurasia during the middle Eocene and terminated in the late Miocene, resulting the intense volcanic activity all of the Eastern Anatolia (Yılmaz et al., 1998; Şengör et al. 2008). The activity was marked during the late Miocene-Pliocene period as the whole plateau is blanket in volcanic rocks, but the first manifestations are intercalated with the middle-late Miocene continental deposits (Yılmaz et al., 1998).

The collision (convergence) began at the ocean-continent boundary and terminated with the continent-continent boundary. This is accommodated by the crustal shortening and the consequent uplift of the Eastern Anatolia High Plateau in terms of deformation (Yılmaz et al., 1998), as a result of which tectonic slices formed through the Eastern Anatolia, and an accretionary complex developed. This complex tectonic feature of the ocean-continent and continent-continent amalgamation is known as the Bitlis-Zagros Suture Zone (Bozkurt, 2001). The northward terrain of the Bitlis-Zagros Suture Zone is underlain by ophiolitic and metamorphic rocks from the late Cretaceous to Oligocene, known as the East Anatolian Accretionary Complex (Şengör et al., 2008). These lead upward to olistrostrome-flysch association of Paleocene-Eocene age and the first manifestations of the volcanic activity (Şengör and Yılmaz, 1981; Yılmaz et al., 1998). The collisional vulcanicity initiated to accompany the crustal shortening-uplift in the late Miocene and acted the whole plateau during the late Miocene-Pliocene period (Yılmaz et al., 1998; Şengör et al., 2008).

By the onset of collisional volcanism, the driving uplift mechanism varied from bulge-related to thermally-driven owing to forming decompression melt pools at the beneath of the East Anatolian Accretionary Complex. The reason that young volcanic cones are distinctive features in the Eastern Anatolia is related to decompression melt pools (Şengör et al., 2008). This melting phenomenon likely appears to be heat source of thermal waters in the Eastern Anatolia as well. By active faults of the Eastern Anatolia, there exist different depths of avenues circulating thermal waters as well as heat.

To the continental portray of tectonics given briefly above, The Varto region is settled into the East Anatolian Accretionary Complex, around the conjunction point of NAF and EAF. The Varto region was covered by thick sedimentary and volcanic units deposited from Tertiary to Quaternary (Fig. 3).

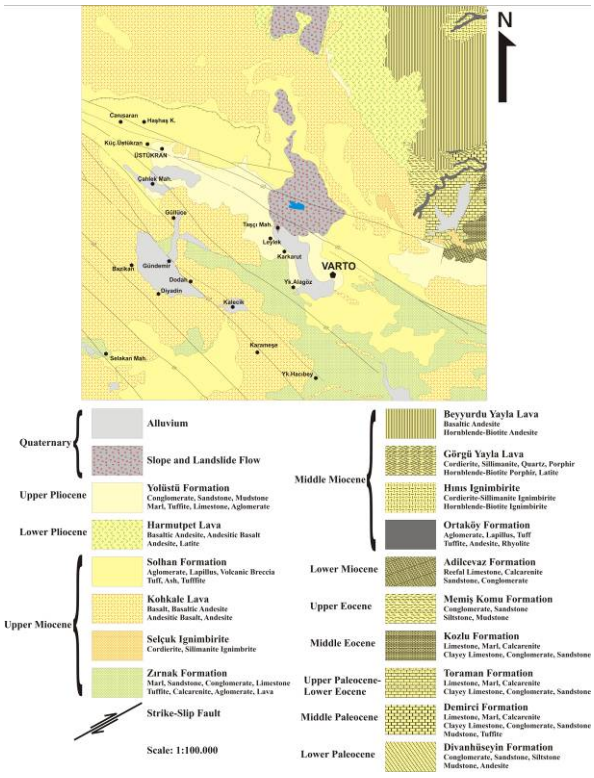

Figure 3: The geological map of the Varto Region.

Rocks aged Lower Paleocene to Upper Eocene, crop out mainly in the northeastern of Varto Region and compose mainly of limestone, conglomerate, sandstone, mudstone of the olistrostrome-flysch association. From Middle Miocene to Upper Pliocene, the succession is represented by volcanic rocks intercalated with continental deposits, both of which cover almost 88% of the total area in the Varto Region. Rock types of the succession mainly compose sandstone, conglomerate, limestone of the sedimentary rock deposits and andesite, tuffite, basalt of the volcanic rocks and are unconformably overlain by Quaternary-aged alluvium, travertine and debris. These types of rocks which are said to be the late Miocene and younger developed in an active tectonic environment of eastern continuation of the NAF (Yılmaz et al., 1998) into the Varto Basin. The age of NAF coincides with the volcanic activity of Upper Miocene. Conjugate pairs of NAF radial lies as NW-SE trending sets in the region (Fig. 3). From the late Miocene to the present, branches of NAF demarcate local basins and the sedimentation developed as well (Şaroğlu and Yılmaz, 1986). The volcanic activity developed as fissure eruptions to the surface through cooling fracture zones extending several meters in depth into local basins delimited by the branches of NAF. Branches of NAF and the fracture zones allow the groundwater circulation in shallow and deep avenues of the depth; also different portions of the circulation depth reflect representing the hydrogeochemical data in connection with water types.

5. REPRESENTING THE HYDROGEOCHEMICAL DATA

The preliminary evaluation of geological conditions of the site provides some information regarding depths of water circulation, bearing potential of the rocks and their influences on the chemistry of springs. To represent the chemistry of the site, twenty springs were sampled, including five hot water springs, two mineral water springs and peripheral water springs (Fig. 4).

Figure 4: Distribution of springs of the site (not to scale).

Red labeled samples, according to surface discharge temperatures, are geothermal type waters; the other ones are mineral and peripheral waters. Measured and chemical parameters are shown in Table 1 and summarized below.

The average discharges of hot water springs in the study area are between 1 to 5L/sec. Surface temperatures of these springs vary 22.5 to 32ºC, electrical conductivity (EC) values from 2100 to 5775 µS/cm. The average discharges of mineral waters in that site are between 0.5 to 2 L/sec. Surface temperatures of them were measured as 13.2 and 14.8ºC. Their electrical conductivity values are also in the range of 719 - 751 µS/cm. The average discharges of cold water springs in the study area are between 1 - 150 L/sec. Surface temperatures of these springs change between 4.9-11.7ºC and electrical conductivity values 51 - 199 µS/cm. Regarding pH values, water samples belonging to the site are entirely distinguished into the pH range of ~5.4 - ~6.2 for hot and mineral waters, ~6.2 - ~7.7 for cold waters. Hot water springs have acidic character, whereas pH values of cold water springs change from slightly acidic, neutral to slightly basic. The ranges of physical parameters measured are affected by outcropping rocks and structural features of the site allowing different portions of the circulation depth.

In the vicinity of the study field, volcanic and sedimentary rocks outcrop. The groundwater flow in the volcanic rocks is controlled by the presence of structural features as suggested by the alignment of the springs, yet not exhaustive information was available as to the circulation depth of groundwater. The information pointing out the circulation depth only arises from alignments of the springs. Thermal, mineral and peripheral water springs discharges from rocks of Upper Miocene and Upper Pliocene (Yolüstü Formation of Upper Pliocene, Kohkale Lava and Zırnak Formation of Upper Miocene in Fig. 3).

These rocks include volcanic rocks and volcanic rocks intercalated with continental deposits; therefore, they are water bearing formations. In addition to this, NAF with Upper Miocene rocks easily mark structural developed avenues of groundwater. Shallow and deep avenues of the groundwater reflect the chemistry of the springs.

Regarding the chemistry of the springs, Schoeller and Piper diagrams are used to classify. Both diagrams give not only information about different water types of the site but also their evolution. For comparing the thermal waters with mineral and peripheral waters, Cl-SO_4-HCO_3 ternary plot was used. This diagram covers the entire spectrum of naturally occurring waters from virtually pure chloride, over mixed chloride-sulfate, to bicarbonate (Giggenbach, 1988; Nicholson, 1993). For the hydrogeochemical data, relative portions of Cl-SO_4-HCO_3 cluster into steam-heated/ condensates and dilute Cl-HCO_3 sectors (Fig. 5), not separated each other except for the data labeled 2.

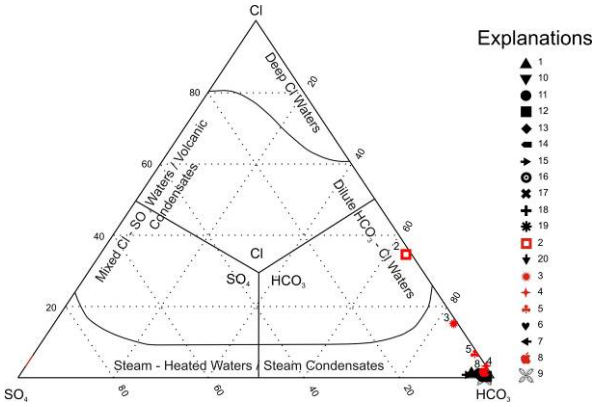

Figure 5: Cl-SO_4-HCO_3 ternary plot with the site data (modified Giggenbach, 1988 and Nicholson, 1993).

The data was plotted on Schoeller and Piper diagrams in doing so dissimilarities with each other could be visible (Fig. 6).

According to Schoeller diagram, peripheral waters can be distinguished easily with low major cations and chloride when comparing with geothermal and mineral waters. According to Piper diagram and the water type classification for it (Deutsch, 1999), thermal springs fall into Na-HCO_3-Cl and Ca-Na-HCO_3 types; mineral and cold waters fall into Ca-HCO_3 type. The hydrogeochemical facies map of the site is shown in Fig. 7. As seen in Fig. 7, the lower altitudes are virtually represented with geothermal waters and the zone of Na-HCO_3-Cl. Cold waters discharge in the higher altitudes and they represent the zone of Ca-HCO_3. In a reasonable way, thermal and mineral waters originates from cold waters with shortcut routes.

When taking account of linear arrangement of plotted data in Fig. 5 and the processes of steam heated and dilution with chloride acting upon them, it is reasonable that peripheral waters descends with rising temperature; therefore, water types are to change from dominant Ca and HCO_3 ions to dominant Na and Cl ions as expressed in Eq. 1.

$$\text{Ca-HCO}_3 \rightarrow \text{Ca-Na-HCO}_3 \rightarrow \text{Na-HCO}_3\text{-Cl} \qquad (1)$$

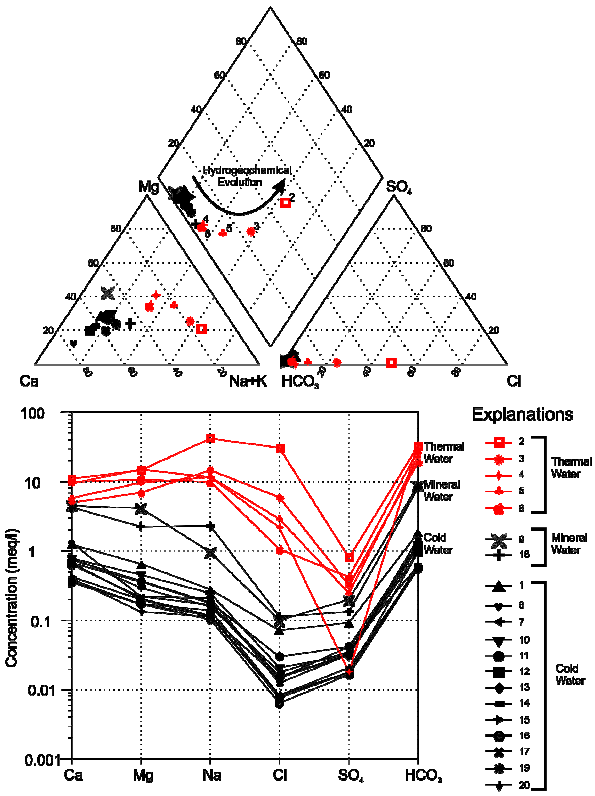

Figure 6: Piper and Schoeller diagrams with the data.

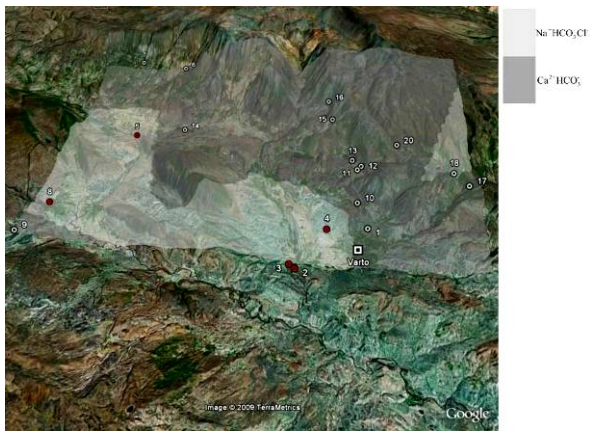

Figure 7: The hydrogeochemical facies map of the site (not to scale).

It can be said that Na and Cl ions are fed from the volcanic rocks. Consequently, volcanic rocks of the site likely appears to be the host rock owing to enrichment of Na and Cl ions in water and abundance of those in minerals of the volcanic rocks. In addition, it is clear that thermal waters have relatively deeper avenues for the circulation than peripheral water under the assumption that they are ascending fluids which deep processes (water-rock interaction, boiling, and steam heating; see Nicholson, 1993 for details) do not affect their isotopic compositions and originate from descending peripheral waters. In other words, thermal waters are meteoric waters and not influenced by deep processes. To support this view, $\delta^{18}O$ (‰), δD (‰), ^3H compositions of selected samples in the site was used.

6. ISOTOPIC COMPOSITIONS OF THE SAMPLES

$\delta^{18}O$ (‰), δD (‰) compositions of the selected samples are essential to explore about whether or not they are meteoric and processed waters. Craig (1961) demonstrated that meteoric waters (precipitation, river and lake samples from various countries) fit on a line known as global meteoric water line (GMWL) represented by the formula in Eq.2.

$$\delta D = 8\delta^{18}O + 10 \quad (2)$$

However, $\delta^{18}O$ and δD values at any locality are strongly dependent upon distance from ocean (continental effect), latitude and altitude (Nicholson, 1993). Thereby, regional (RMWL), expressly local meteoric water lines (LMWL) are convenient references for understanding local groundwater isotopic variations reference to local meteoric waters (Mazor, 2004). Isotopic signatures of groundwater can shift from meteoric water lines to schematic trends designating processes; each process signs a shift in isotopic composition to the extent that δD as well as $\delta^{18}O$ enrich. Isotopic processes can be separated as surficial and deep processes including surface evaporation for the former; water-rock interaction, steam heating and boiling for the latter respectively. Groundwater influenced by these processes is defined as processed water mentioned in the first line of this section. To explore that whether the selected samples are processed or not, selected RMWL (Gat, 1983; Eisenlohr, 1995) and LMWL (Sayın and Eyüpoğlu, 2005) are used (Eq. 3) and the site data given in Table 2 are plotted (Fig. 8).

$$\begin{aligned}
&\delta D = 8\delta^{18}O + 22.00 \text{ (Eastern Mediterranean)}\\
&\delta D = 8\delta^{18}O + 16.00 \text{ (Marmara)}\\
&\delta D = 8\delta^{18}O + 10.00 \text{ (Global \& Central Anatolia)}\\
&\delta D = 8\delta^{18}O + 11.36 \text{ (Dalbahçe-Erzurum)}\\
&\delta D = 8\delta^{18}O + 14.87 \text{ (Şenyurt-Erzurum)}
\end{aligned} \quad (3)$$

The data are separated as thermal and cold waters in the diagram and clustered between RMWL of Eastern Mediterranean and Marmara. Isotopic signatures of the site data have not any trend indicating the processes. Thermal waters of the site are characterized by the very negative $\delta^{18}O$ and δD values. It is thought that this is evidence of different aged waters. To support this view, ^3H values of the selected samples were evaluated.

Table 2: $\delta^{18}O$ and δD values of the selected samples.

Sample No	$\delta^{18}O$ (‰)	δD (‰)
1	-10.59	-65.86
3	-12.51	-82.50
4	-12.48	-78.47
5	-12.17	-79.81
8	-12.50	-80.41

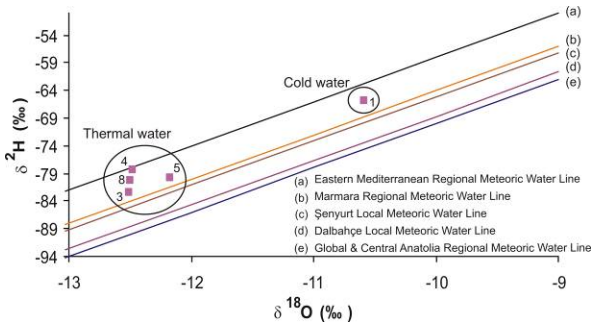

Figure 8: The δD (‰) *vs* $\delta^{18}O$ (‰) diagram.

Their amounts of ^3H give groundwater circulation time consumed, while reaching from recharge to discharge as simply stated that the less ^3H amount groundwater has, the older it is, or the longer avenue it has. This statement is applicable under the assumption of piston flow model (no dispersion or mixing between different aged flow paths; see Kazemi et al., 2006 for details). To this model, the passage of time through which the amount of ^3H decreased can be calculated by the decay law in Eq. 4 (Kresic, 2007).

$$^3H_S = {}^3H_0 e^{-\lambda t} \quad (4)$$

where ^3H_S is the amount of ^3H in the sample, $^3H_0$ is the amount of ^3H in the precipitation, and λ is the decay constant of tritium of 0.056 $year^{-1}$. In this equation, the main important is to determine ^3H amount in precipitation essentially needed for the use of ^3H as a tracer of groundwater circulation time. Therefore, how much ^3H atoms there are in precipitation water should be measured to determine peak values of natural ^3H amount. This type measurements are related to thermonuclear testings started in 1952 (Kazemi et al., 2006). During the tests, large quantities of tritium released into atmosphere; hence, natural ^3H in precipitation between 5 and 20 tritium units (TU), stated by Kaufmann and Libby (1954) reached up to several thousands TU in precipitation (Mazor, 2004). To sum up, the year of 1952, beginning of thermonuclear tests is an indicator to determine pre and post-1952 recharges entering into aquifers. To estimate pre and post-1952 recharges belonging to the site, ^3H values in Table 3 are used. According to Eq. 2, it is not realistic to calculate groundwater circulation time because of sensitive to mixing of different aged waters and not exhaustive information about ^3H amounts of prior or present precipitations. In the calculation with Eq.2, 3-6 TU values offered for Europe by Solomon and Cook (2000) were used.

Table 3: ^3H values of the selected samples.

Sample No	^3H Values (TU)
1	6.40±0.80
3	0.40±0.65
4	0.00±0.60
5	0.95±0.65
8	0.20±0.65

The results sign post-1952 recharges for all samples, but this is unrealistic because thermal waters may mix with cold waters before being discharged in a spring or well (Nicholson, 1993). To overcome this informative gap, a semi-quantitative method (Yıldız et al. 2008) and a classification (Kazemi et al., 2006) were used to differentiate pre and post-1952 recharges. ^3H values less than 6 TU indicates mixing of pre and post-1952 recharges, whereas the values more than 6 TU is a sign for post-1952 recharges. Except for the spring labeled 1 which indicates cold water (post-1952), all thermal waters are mixed with cold waters. In conclusion, in spite of being known that thermal water samples cluster into steam-heated /condensates and dilute $Cl\text{-}HCO_3$ sectors in $Cl\text{-}SO_4\text{-}HCO_3$ ternary plot (Fig. 5), there is no evidence as to shifting from meteoric water lines. Therefore, steam-heated condition is available for the site but robust checking for it, solute geothermometers were used. It was expected that the host rock temperature are lower than steam condensate conditions.

7. APPLICATION OF GEOTHERMOMETERS FOR THE SITE DATA

Chemical analyses of geothermal fluids can be used to estimate subsurface reservoir temperature. Chemical geothermometers depend on water–mineral equilibria and give the last equilibration temperature for the reservoir (see Nicholson, 1993 for the list and a discussion). All are based on the premise that a temperature-dependent water-mineral equilibrium is attained in the reservoir. Chemical geothermometry techniques (Kharaka and Mariner, 1989; Fournier, 1991) were applied to thermal waters in the site. According to solution geothermometers, β-Cristobalite and Li-Mg geothermometers are appropriate (Table 4). For a robust checking, appropriate solution geothermometers given were made clear by providing Giggenbach (1988) and SI diagrams (Reed & Spycher, 1984).

Table 4: Reliable solution geothermometer results.

Geothermometer	Reference	*2	*3	*4	*5	*8
Silica β-Cristobalite	Fournier (1991)	54	55	55	70	80
Li-Mg	Kharaka & Mariner (1989)	66	54	54	54	44

* All calculated values are in ºC.

The ternary plot of Na/1000–K/100–$Mg^{1/2}$ of Giggenbach (1988) is a method to discriminate mature waters which have attained equilibrium with relevant hydrothermal minerals from immature waters and waters affected by mixing and/or re-equilibration at low temperatures during their circulation (Fig. 9).

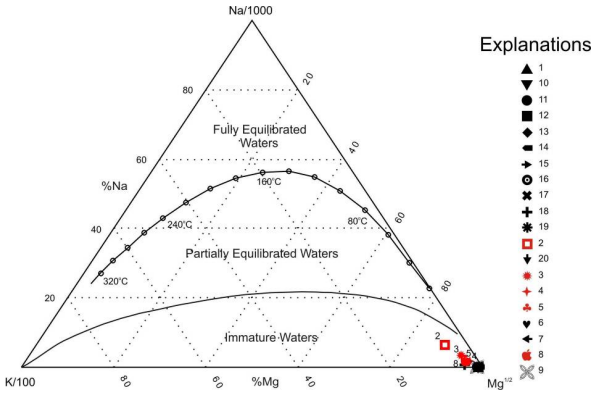

Figure 9: The Giggenbach diagram with plotted data.

All samples are plotted into immature water zone in Fig. 9. Reservoir temperature values estimated by this method are not valid, because thermal waters mix with some portions of peripheral (cold) and mineral water. As a result of which Na-K geothermometers show unacceptable results for groundwater samples in this site.

A different approach to geothermometry (Reed & Spycher, 1984) is illustrated in Fig. 10, where the changes in SI of relevant minerals with temperature were investigated for the thermal water samples of the site.

In the calculation of the mineral saturation indices of the waters in the study field, PhreeqC code (Parkhurst and Appelo, 1999) was used. It is observed that the geothermal fluids are saturated with dolomite, calcite and aragonite minerals. According to these data, it is possible to report that the reservoir temperature of the geothermal fluids is between 50ºC and 80ºC. Fig. 8 shows SI for selected minerals *vs* T for thermal waters of the site. According to Fig. 8, the reservoir temperatures estimated by this method are 55°C for sample 2, 60°C for sample 3, 50°C for sample 4, 80°C for sample 5 respectively. Due to not coinciding at SI zero axis for sample 8, the method does not allow a good estimation of reservoir temperature for it.

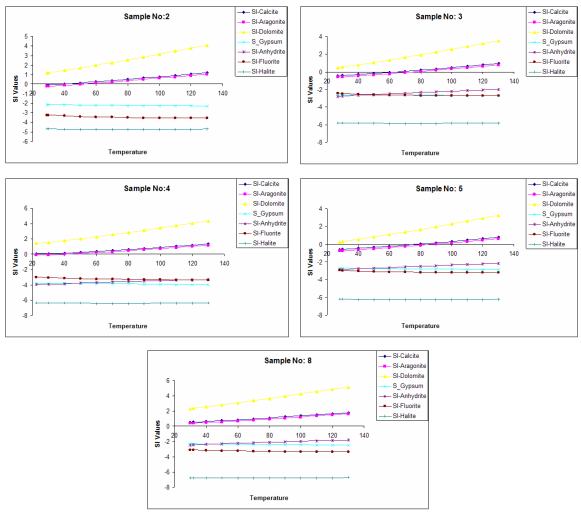

Figure 10: SI for selected minerals vs T for thermal waters of the site.

In conclusion, host rock temperature results are lower so exceptionally coherent with $\delta^{18}O$ and δD values indicating no deep process or shifting form meteoric water lines. Hence, thermal water springs are likely heated by steam.

8. CONCLUSION

According to the Piper diagram, springs fall into Na-HCO_3-Cl type for thermal waters and Ca-HCO_3 type for cold waters. Due to the fractures allowing deep circulation of groundwater and dominant Na-Cl component, the host rock is probably volcanic origin. Hot waters have the same recharge area with cold waters. Reliable reservoir temperature ranges for hot waters were obtained with Li-Mg geothermometer and β-Cristobalite geothermometer as 44-66ºC and 54 - 80ºC, respectively. These values are also checked with Saturation Indices (SI) *vs* T diagrams. Results of SI *vs* T diagrams indicate equilibriun with calcite and aragonite minerals which gives comparable results with Li-Mg and β-Cristobalite geothermometers. It is possible to get 80°C reservoir temperature by drilling in this area with the help of field observations and the data obtained. The geothermal potential of the study area hadnot been evaluated until now. Utilization of this geothermal district might make a considerable contribution to tourism and agriculture usages.

9. REFERENCES

Bozkurt, E.: Neotectonics of Turkey-A Synthesis, *Geodinamica Acta*, **14**, (2001), 3-30.

Craig, H.: Isotopic Variations in Meteoric Waters, *Science*, **133**, (1961), 1702–1703.

Deustch, W.: *Groundwater Chemistry Fundamentals and Applications to Contamination*, Lewis Publishers, New York, (1997).

Eisenlohr, T.: Die Thermalwässer der Armutlu-Halbinsel (NW-Türkei) und deren Beziehung zu Geologie und Aktiver Tektonik, *PhD. Dissertation*, ETH-Zürich, Nr.11340, (1995).

Fournier. R. O.: Water geothermometers applied to geothermal energy. In: *Applications of Geochemistry in Geothermal Reservoir Development* (co-ord. by F. D'Amore), UNITAR Publ., Rome, Italy, (1991), 37-69.

Gat, J.R.: Precipitation, Groundwater and Surface Waters: Control of Climate Parameters on their isotopic composition and their utilisation as palaeo climatological tools, *Proceedings*, Palaeoclimates and Palaeowaters: A Collection of Environmental Isotope Studies (Proc. Advisory Group Mtg Vienna, 1980), IAEA, Vienna, (1983), 3-12.

Giggenbach, W.F.: Geothermal Solute Equilibria. Derivation of Na-K-Mg-Ca Geoindicators, *Geochimaca et Cosmochimica. Acta*, **52**, (1988), 2749-2765.

Kaufmann, S., and Libby, W.S.: The Natural Distribution of Tritium, *Physical Review*, **93(6)**, (1954), 1337-1344. In: Kresic, N.: *Hydrogeology and Groundwater Modeling*, CRC Press, Taylor & Francis Group, 2nd Edition, USA, (2007).

Kazemi, G.A., Lehr, J.H., Perrochet, P.: *Groundwater Age*, Wiley-Interscience, New Jersey, USA, (2006).

Kharaka, Y.K. and Mariner, R.H., Chemical Geothermometers and Their Application to Formation Waters From Sedimentary Basins. In: Neaser, N.D. and McCollon, T.H. (eds.): Thermal History of Sedimentary Basins, Springer-Verlag, New York, (1989), 99-117.

Kresic, N.: *Hydrogeology and Groundwater Modeling*, CRC Press, Taylor & Francis Group, 2nd Edition, USA, (2007).

Mazor, E.: *Applied Chemical and Isotopic Groundwater Hydrology*, Marcel Dekker, Inc, 3rd Edition, New York, (2004).

Nicholson, K.: *Geothermal Fluids Chemistry and Exploration Techniques*, Springer-Verlag, Berlin, (1993).

Parkhust, D.L. and Appelo, C.A.J.: User's guide to PHREEQC (Version2)- A Computer Program for Speciation, Batch Reaction, One Dimensional Transport and Inverse Geochemical Calculations-, *Water Resources Investigation Report 99-4259*, Denver-Colorado, (1999).

Reed, M. and Spycher, N.: Calculation of pH and mineral equilibria in hydrothermal waters with application to geothermometry and studies of boiling and dilution, *Geochimaca et Cosmochimica. Acta*, **48**, (1984), 1479-1492.

Sayın, M., and Eyüpoğlu, S.,Ö.: Determination of The Local Meteoric Water Lines Using Stable Isotope Contents of Precipitation In Turkey (in Turkish), *Proceedings*, II. National Symposium of Isotopic Methods in Hydrology, General Directorate of State Hydraulic Works, İzmir, (2005), 323-344.

Solomon, D. K., and Cook, P. G.: ^{3}H and ^{3}He. In: Cook, P. G., and Herczeg, A. L. (eds.): *Environmental Tracers in Subsurface Hydrology*, Kluwer Academic Publishers, Boston, (2000), 397-424.

Şaroğlu, F., and Yılmaz, Y.: Geological Evolution and Basin Models during The Neotectonic Episode in Eastern Anatolia, *MTA Bulletin*, **107**, (1986), 61-83.

Şengör, A.M.C., and Yılmaz, Y.: Tethyan Evolution of Turkey: A Plate Tectonic Approach, *Tectonophysics*, **75**, (1981), 181-241.

Şengör, A.M.C., Özeren, S., Keskin, M., Sakınç, M., Özbakır, A.D., Kayan, İ.: Eastern Turkish High Plateau as A Small Turkic-Type Orogen: Implications for Post-Collisional Crust-Forming Processes In Turkic-Type Orogens, *Earth-Science Reviews*, **90**, (2008), 1-48.

Şimşek, Ş.: Geothermal Potential of Turkey, *Marmara Poly Project*, VDF, (1997), 111-125.

Yıldız, F.E., Dilaver, A.T., Gürer, İ., Ünsal, N., Bayarı, S., Türkileri, S., Çelenk, S.: Determination of Groundwater-Surface water Relation in Develi Closed Basin by Using Environmental Isotopes (in Turkish), *Proceedings*, III. National Symposium of Isotopic Methods in Hydrology, General Directorate of State Hydraulic Works, İstanbul, (2008), 25-35.

Yılmaz, Y., Güner, Y., Şaroğlu, F.: Geology of The Quaternary Volcanic Centers of The East Anatolia, *Journal of Volcanology and Geothermal Research*, **85**, (1988), 173-210.

Table 1: Chemical and measured parameters.

Sample No	Easting	Northing	Elevation (m)	T (ºC)	Q (l/s)	EC (µS/cm)	pH	Type	Na (ppm)	K (ppm)	Mg (ppm)	Ca (ppm)	HCO_3 (ppm)	Cl (ppm)	Li (ppm)	SO_4 (ppm)	Si (ppm)
1	712506	4339901	1573	11.6	3	187	6.22	Cold	6.34	2.44	7.82	25.03	110.91	2.55	0.00	4.40	28.4
2	708927	4337029	1465	29	3-5	5775	6.04	Thermal	970.00	77.15	177.38	218.69	1971.72	1076.99	1.26	38.70	61.8
3	708625	4337352	1434	26.8	5	2100	6.09	Thermal	335.25	30.35	83.48	100.42	1139.04	208.93	0.50	15.26	63.2
4	710407	4339752	1497	22.5	1-2	2845	6.19	Thermal	269.07	25.78	182.74	189.52	2069.68	77.31	0.75	0.86	62.9
5	697835	4346054	1520	28.2	1	2155	5.75	Thermal	269.04	30.99	118.06	115.20	1391.91	102.94	0.60	11.89	80.0
6	699782	4352013	2072	8.9	2	77	7.72	Cold	3.85	0.84	2.67	26.49	89.34	0.55	0.00	1.56	14.4
7	696479	4352499	2050	8.6	50	61	7.09	Cold	2.64	1.14	2.10	7.08	33.89	0.27	0.00	0.86	16.4
8	694874	4339601	1472	32		2334	6.06	Thermal	225.05	34.00	131.36	200.65	1688.28	37.44	0.40	20.09	93.0
9	694153	4337217	1524	14.8	2	751	6.16	Mineral	22.13	6.07	50.52	90.75	532.98	3.53	0.02	9.54	50.1
10	711941	4341403	1659	11	1-2	136	6.50	Spring	5.66	1.89	5.57	15.72	77.02	0.75	0.00	1.50	28.4
11	711876	4343505	1848	10.3	2.5	115	6.54	Cold	4.12	2.30	4.47	14.87	73.94	1.06	0.00	2.00	20.2
12	712072	4343678	1910	7.2		60	6.68	Cold	2.68	1.23	2.47	13.22	58.60	0.28	0.00	0.83	15.9
13	711587	4344202	1857	9.2	1	105	6.73	Cold	4.08	1.29	4.38	13.28	70.92	0.53	0.00	1.49	22.6
14	700947	4346658	1936	9.2	1.8	90	6.93	Cold	3.68	1.36	3.58	16.07	67.78	0.63	0.00	1.67	19.4
15	710297	4346997	2089	6.7	1	63	7.09	Cold	2.63	1.55	2.41	8.45	36.91	0.51	0.00	2.03	16.9
16	709989	4348552	2147	4.9		51	7.34	Cold	2.35	1.06	2.08	7.06	33.83	0.23	0.00	0.78	14.5
17	717689	4342614	1940	7.5	1.5	87	7.11	Cold	4.78	0.97	2.60	12.69	58.54	0.44	0.00	1.55	17.0
18	717105	4343680	1901	13.2	0.5	719	5.41	Mineral	52.80	18.58	27.47	84.29	499.09	4.05	0.06	6.44	56.9
19	717105	4343680	1901	6	150	63	7.30	Surface	3.24	1.38	2.08	7.53	36.91	0.29	0.00	0.85	15.8
20	713930	4344827	2120	5.4	1.5	52	6.42	Cold	2.59	1.34	1.61	8.08	33.89	0.29	0.00	0.99	14.3